Physisorption-Induced C-H Bond Elongation in Methane

H. Öström,[1,2] H. Ogasawara,[3] L.-Å. Näslund,[1] L. G. M. Pettersson,[1] and A. Nilsson[1,3,*]

[1]*Stockholm University, AlbaNova University Center, Fysikum, SE-106 91 Stockholm, Sweden*
[2]*Fachbereich Physik, Freie Universität Berlin, Arnimallee 14, D-14195 Berlin-Dahlem, Germany*
[3]*Stanford Synchrotron Radiation Laboratory, Post Office Box 20450, Stanford, California 94309, USA*

(Received 19 December 2005; published 13 April 2006)

Physisorption of methane to a Pt surface was studied by x-ray absorption spectroscopy in combination with density functional theory spectrum calculations. The experiment shows new electronic states appearing upon physisorption. We find that these states are due to orbital mixing causing charge polarization as a means to minimize Pauli repulsion. The results can be explained by elongation of 1 C-H bond by 0.09 Å in the physisorbed state even though no covalent chemical bond is formed.

DOI: 10.1103/PhysRevLett.96.146104 PACS numbers: 68.43.−h, 82.45.Jn, 82.65.+r

The activated dissociation of methane at metal surfaces is the rate-limiting step in steam reforming [1], which is the principal process for hydrogen production in industrial catalysis. Methane adsorption at single-crystal metal surfaces has often been used as a well-defined model system to study this important reaction. Saturated hydrocarbons are weakly adsorbed and conventionally no electronic interaction has been anticipated for the adsorbate systems, except at certain sites like kinks [2] where the molecules can bind more strongly. However, recent studies have shown that the electronic and geometric structure of larger alkanes can change upon adsorption [3,4], even at noble metal surfaces.

Methane desorbs intact from the Pt(111) surface upon heating [5]. However, recently molecular beam experiments [6–13] have shown that methane dissociation at surfaces can be activated by kinetic energy equally well as by vibrational energy added to the incident methane. The dissociation of adsorbed methane can also be activated already below room temperature at high pressure [14] or by irradiation using 193 nm (6.4 eV) photons [5,15], at which wavelength methane is transparent in the gas phase [16,17]. Reliable theoretical studies of the adsorption based on total energy calculations are difficult due to the lack of dispersion forces in the density functional theory (DFT) methods commonly employed. On Ni, which is an efficient dehydrogenation catalyst, no computed energy minimum at all is found for methane adsorption with DFT calculations [18]. There is thus a need for additional experimental data to answer the question: How does the metal surface change the electronic structure of the molecule to facilitate dissociation?

In the present work we measured the unoccupied local electronic structure of the carbon in adsorbed methane using angular resolved x-ray absorption spectroscopy (XAS), which probes the atom-projected unoccupied local p density of states in a way that allows us to separate electronic states of different atomic p symmetry. The experiments were performed at the undulator beam line 8.0 at the Advanced Light Source at Lawrence Berkeley National Laboratory. The experimental end station has a base pressure below 10^{-10} torr and houses a Scienta SES-100 electron spectrometer for x-ray photoelectron spectroscopy (XPS) as well as a partial electron yield detector for XAS. The Pt(977) crystals were mounted at 10° grazing incidence and were rotatable around the axis of the incoming photon beam allowing for different orientations of the E vector of the incoming light relative to the surface. The sample cleanliness was checked with low energy electron diffraction and XPS after cycles of argon ion sputtering and annealing to 1000 K. The methane layer was prepared at a substrate temperature of 40 K and the presence of a pure molecular phase without any dissociated species was confirmed with XPS. The sample was scanned continuously during measurements in order to avoid beam damage. The measured spectra contain contributions from at most 3% damaged molecules as quantified by XPS and by recording several XA spectra on the same sample area; this is well within the error bars of our analysis. The XAS signal was divided by the flux of the incoming photon beam as recorded on a gold mesh in the beam line. Contributions from the clean sample signal were subtracted out, after normalization before the absorption onset, to yield the final XA spectra. The monochromator energy was calibrated using the Pt Fermi level, where the difference in the measured photon energies for the first and second order diffracted light gives the correct monochromator energy.

Spectrum calculations were performed using the STOBE-DEMON DFT code. The adsorption system was modeled with either one or seven methane molecules on top of a Pt_{10} cluster consisting of two layers with 7 and 3 atoms, forming a Pt(111) surface; the positions of the Pt atoms were constrained to those of bulk Pt. For the 1-methane clusters no symmetry was used, whereas for the 7-methane cluster, C_3 symmetry was used to reduce the cost of the calculations. All XA spectra were computed for only the methane molecule at the center of the cluster in order to avoid edge effects. All metal atoms were described using 16-electron relativistic effective core potentials. The XA spectra were computed in the dipole approximation using the transition potential approach [19,20]. For a comparison with experiment the computed spectra were shifted 2.3 eV towards lower energy and broadened with 0.7 eV Gaussian functions below the ionization level and linearly increasing width above it.

The lowest unoccupied molecular orbital (LUMO) in gas-phase methane is the totally symmetric $3a_1$, which is symmetry forbidden in C 1*s* XAS. A gas-phase methane XA spectrum from Ref. [21] is shown with a solid line at the bottom of Fig. 1. The spectrum shows a main peak at 288.0 eV corresponding to the triply degenerate $2t_2$ LUMO + 1 orbital followed by vibrational progression and Rydberg orbitals at higher energy. In addition, a small feature, corresponding to transitions into the symmetry-forbidden $3a_1$ LUMO orbital, appears at 286.9 eV due to vibronic coupling. The top and middle solid line spectra in Fig. 1 were recorded for a saturated monolayer methane adsorbed at a Pt(977) surface. The Pt(977) surface is a stepped (111) surface, where approximately 10% of the atoms are step atoms. Although steps promote the activated dissociation of methane [22], we did not observe any significant effect from the steps in our coverage dependent low temperature adsorption experiments and our analysis will consequently only deal with terrace adsorption sites. More details are given in Ref. [20].

The middle solid line spectrum in Fig. 1 was recorded with the *E* vector of the incoming light in the surface plane, selectively probing orbitals with *p* character pointing along this direction. This spectrum shows the same main features as the gas-phase spectrum, but it is broadened through the interaction with the metal surface. The topmost solid line spectrum in Fig. 1 shows the adsorbate XAS recorded with the *E* vector perpendicular to the surface plane. This spectrum shows the same features as the in-plane spectrum, but in addition the symmetry-forbidden gas-phase LUMO orbital, denoted "A_1" in Fig. 1, becomes visible due to the symmetry being broken at the metal surface [23], which allows the orbital to gain *p* character by mixing with higher-lying orbitals. There is also a broad band denoted M^* ranging from the gas-phase LUMO all the way down to the Fermi level. The position of the Fermi level is shown by the inset XP spectrum. The M^* band is due to the interaction with the metal and is similar to adsorption-induced states previously observed for adsorbed long-chain alkanes [24–26].

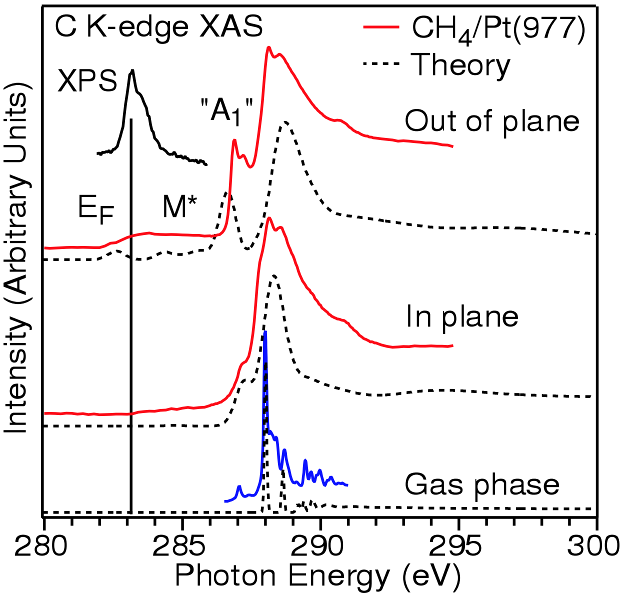

FIG. 1 (color online). Experimental x-ray absorption spectra of methane adsorbed on a Pt surface. The solid lines show from the top: methane adsorbed on a Pt(977) surface taken with the *E* vector out of the surface plane, *E* vector in the surface plane, and gas-phase methane from Ref. [21]. The dashed lines show the corresponding computed spectra, shifted 2.3 eV towards lower energy to match the experimental energy scale. An x-ray photoelectron spectrum is shown to give the position of the Fermi level.

Calculations of XA spectra within the DFT framework were performed both for a single molecule and methane adsorbed on a Pt_{10} cluster with a (111) surface for several different molecular geometries. No total energy geometry optimization was performed for the adsorbate system since the total energy is not reliable due to the lack of dispersion interaction, which is important for weakly adsorbed systems [27]. Instead, the XA spectral features, which are very sensitive to the local geometry, were used for determination of the adsorption geometry; the calculations reproduce both the appearance of the gas-phase symmetry-forbidden $3a_1$ state as well as the metal-induced states above the Fermi level. In the calculations methane was adsorbed with only one hydrogen atom pointing toward the surface and with adsorbate-adsorbate interaction taken into account, as shown in the bottom panel of Fig. 2; alternative structures resulted in less satisfactory agreement. To get good quantitative agreement, which can be expected based on previous work [3,28], several calculations were performed where the molecule-metal (C-Pt) distance and the distance between the carbon and hydrogen atom pointing towards the surface ($C\text{-}H_d$) were changed independently in a two-dimensional space. Relaxation of the rest of the hydrogen atoms was performed for a few cases and leads to a slight flattening of the molecule, as can be expected when weakening a C-H bond. This small relaxation had no significant effect on the resulting spectra and was therefore not taken into account in the analysis. The main effects when changing the $C\text{-}H_d$ and C-Pt distances are, first, the relative intensity of the region between the Fermi level and symmetry-forbidden peak with respect to the main peak and, second, the splitting between the peak corresponding to the symmetry-forbidden state and the main peak. Spectra corresponding to a few computed geometries are shown in Fig. 2. Calibration calculations with the gas-phase methane molecule showed that the transition potential approach used in this work gives a 50% larger splitting than the experimental value and that state-by-state [29] calculations resolve this discrepancy by a more accurate treatment of relaxation effects [19]. The symmetry-

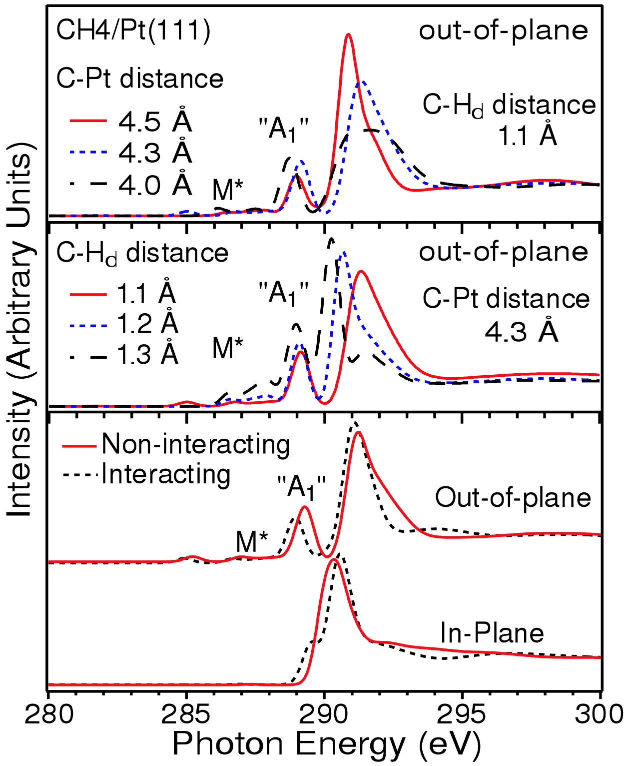

FIG. 2 (color online). C-H_d and C-Pt distance dependence of the XA spectra. The top panel shows the out-of-plane computed XA spectra as a function of C-Pt distance. The middle panel shows the out-of-plane XA spectra as a function of C-H_d distance and the bottom panel shows the out-of-plane and in-plane XA spectra both with and without neighboring methane molecules in the model.

forbidden state is dipole forbidden in the equilibrium geometry used in the calculations and is thus only present with zero intensity. These more accurate calculations are, however, too demanding to perform for the adsorbate system and instead the transition potential (TP) approach was used under the assumption that it produces a too large splitting by the same scale factor also for the adsorbed species. Because of the still relatively weak interaction we do not expect any significant change in this scaling when going from the gas-phase molecule to the adsorbate; a difference in splitting between TP and experiment similar to that for gas phase is thus appropriate for the adsorbate (Fig. 1, top). The geometry that gives the best fit is one where 1 C-H bond is stretched 8% of the original bond length from 1.09 Å to 1.18 ± 0.05 Å with the molecule at a distance of 4.15 ± 0.1 Å between the C and closest Pt atom and the corresponding spectra are shown in Fig. 1. We monitored the relative computed total energies for changes in the geometry, as well as through a constrained space orbital variation analysis [30]. The obtained total energy differences are smaller than 0.1 eV, which is within the error bars of the technique. The computed energy cost of the geometry distortions is thus small enough to be compensated by dispersion interactions that are not included in the theory.

Figure 3 shows the charge density difference between the adsorbate system and the separated molecule and cluster. This is an established type of analysis, which can be used [3,28,31] to deduce electron rearrangements upon interaction with the surface. The charge density difference is plotted in Fig. 3 along a plane containing the C and H_d atoms of the methane molecule as well as a row of first-layer Pt atoms, as shown in the lower part of the figure. Solid lines in the plot denote electron charge buildup and dashed lines denote charge depletion. We note an increase of charge at the C and a decrease at the H_d atom in the adsorbed methane, showing a polarization away from the surface. At the metal atoms there is a corresponding polarization of charge towards the methane molecule. In addition, there is only very little charge increase between the molecule and metal. We interpret this as no electron pairing being formed, since this is less than 2% of the change observed upon formation of, e.g., a covalent H-H bond. The electronic structure is, however, significantly affected by the presence of the metal as shown by the experimental XAS data. Upon adsorption the C-H_d bonding and antibonding orbitals mix due to interaction with the metal surface and induce a polarization away from the surface to minimize the Pauli repulsion, while the metal responds by forming an image charge resulting in charge polarization towards the molecule. This mixing gives rise to the new M^* band in the absorption spectrum due to formation of three-center C-H-M orbitals similar to the

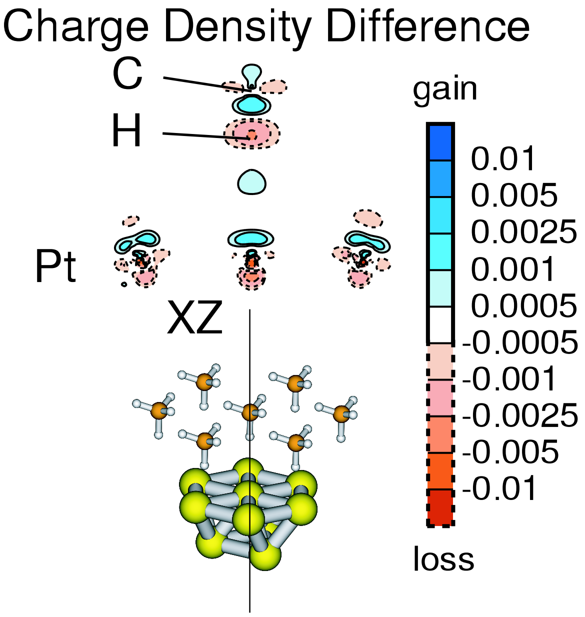

FIG. 3 (color online). Charge density difference of methane upon adsorption on a Pt surface. Solid and dashed lines denote increased and decreased electron density, respectively. The lower part of the figure shows the cutting plane, which contains the C and the closest Pt atoms.

case of octane adsorption on Cu(110) [3], where the M* feature is essentially the nonbonding orbital. The appearance of a new adsorbate absorption band between the gas-phase highest occupied molecular orbital and LUMO correlates well with the observation that adsorbed methane can be dissociated by 193 nm (6.4 eV) light through a direct photo excitation, even though gas-phase methane is transparent at this wavelength.

The charge polarization leading to C-H elongation also gives a consistent explanation to the strong dependence on incident kinetic energy of methane dissociation in molecular beam experiments of methane [9,12]. Molecules with larger incident kinetic energy are pushed further into the repulsive barrier and thus respond with a larger polarization of the electron density away from the metal in order to minimize the Pauli repulsion, leading to an increased elongation of the C-H bond and subsequent dissociation. The C-H bond elongation, which occurs already in the physisorbed state, can thus be viewed as a precursor step to the dissociation. For this pathway to be active at the Pt surface the interaction does, however, need to be enhanced, e.g., by incident kinetic energy or interaction above the desorption temperature as in high-pressure experiments or with scattering of vibrationally excited molecules.

In conclusion, our combined XAS and DFT study shows unoccupied states appearing between the Fermi level and the gas-phase LUMO due to mixing between bonding and antibonding C-H orbitals, leading to a significant bond elongation (~ 0.09 Å). Although methane is only physisorbed on the Pt substrate we interpret this as a first step towards C-H activation and dehydrogenation and determine the mechanism behind the bond elongation to be minimization of Pauli repulsion, rather than formation of a surface chemical bond.

This work was supported by the Swedish Foundation for Strategic Research, the Swedish Natural Science Research Council and the U.S. Department of Energy, Office of Basic Energy Sciences through the Stanford Synchrotron Radiation Laboratory and the Advanced Light Source. We would like to acknowledge Jonathan Denlinger at beam line 8.0, Advanced Light Source, for valuable assistance.

---

*Corresponding author.
Email address: nilsson@slac.stanford.edu

[1] H. S. Bengaard, J. K. Nørskov, J. Sehested, B. S. Clausen, L. P. Nielsen, A. M. Molenbroek, and J. R. Rostrup-Nielsen, J. Catal. **209**, 365 (2002).

[2] G. Henkelman and H. Jónsson, Phys. Rev. Lett. **86**, 664 (2001).

[3] H. Öström, L. Triguero, M. Nyberg, H. Ogasawara, L. G. M. Pettersson, and A. Nilsson, Phys. Rev. Lett. **91**, 046102 (2003).

[4] H. Öström, L. Triguero, K. Weiss, H. Ogasawara, M. G. Garnier, D. Nordlund, L. G. M. Pettersson, and A. Nilsson, J. Chem. Phys. **118**, 3782 (2003).

[5] Y. A. Gruzdkov, K. Watanabe, K. Sawabe, and Y. Matsumoto, Chem. Phys. Lett. **227**, 243 (1994).

[6] R. D. Beck, P. Maroni, D. C. Papageorgopoulos, T. T. Dang, M. P. Schmid, and T. R. Rizzo, Science **302**, 98 (2003).

[7] T. P. J. Beebe, D. W. Goodman, B. D. Kay, and J. T. J. Yates, J. Chem. Phys. **87**, 2305 (1987).

[8] P. M. Holmblad, J. Wambach, and I. Chorkendorff, J. Chem. Phys. **102**, 8255 (1995).

[9] M. B. Lee, G. Y. Yang, and S. T. Ceyer, J. Chem. Phys. **87**, 2724 (1987).

[10] A. C. Luntz and D. S. Bethune, J. Chem. Phys. **90**, 1274 (1989).

[11] C. T. Rettner, H. E. Pfnür, and D. J. Auerbach, Phys. Rev. Lett. **54**, 2716 (1985).

[12] M. B. Lee, Q. Y. Yang, S. L. Tang, and S. T. Ceyer, J. Chem. Phys. **85**, 1693 (1986).

[13] T. Fuhrmann, M. Kinne, B. Tränkenschuh, C. Papp, J. F. Zhu, R. Denecke, and H.-P. Steinrück, New J. Phys. **7**, 107 (2005).

[14] A. L. Marsh, K. A. Becraft, and G. A. Somorjai, J. Phys. Chem. B **109**, 13 619 (2005).

[15] K. Watanabe, K. Sawabe, and Y. Matsumoto, Phys. Rev. Lett. **76**, 1751 (1996).

[16] L. C. Lee and C. C. Chiang, J. Chem. Phys. **78**, 688 (1983).

[17] N. Wainfan, W. C. Walker, and G. L. Weissler, Phys. Rev. **99**, 542 (1955).

[18] P. Kratzer, B. Hammer, and J. K. Nørskov, J. Chem. Phys. **105**, 5595 (1996).

[19] L. Triguero, L. G. M. Pettersson, and H. Ågren, Phys. Rev. B **58**, 8097 (1998).

[20] See EPAPS Document No. E-PRLTAO-96-051616 for details of the calculations. For more information on EPAPS, see http://www.aip.org/pubservs/epaps.html.

[21] J. Schirmer, A. B. Trofimov, K. J. Randall, J. Feldhaus, A. M. Bradshaw, Y. Ma, C. T. Chen, and F. Sette, Phys. Rev. A **47**, 1136 (1993).

[22] A. T. Gee, B. E. Hayden, C. Mormiche, A. W. Kleyn, and B. Riedmüller, J. Chem. Phys. **118**, 3334 (2003).

[23] J. Yoshinobu, H. Ogasawara, and M. Kawai, Phys. Rev. Lett. **75**, 2176 (1995).

[24] K. Weiss, J. Weckesser, and C. Wöll, J. Mol. Struct., Theochem **458**, 143 (1998).

[25] K. Weiss, H. Öström, L. Triguero, H. Ogasawara, M. G. Garnier, L. G. M. Pettersson, and A. Nilsson, J. Electron Spectrosc. Relat. Phenom. **128**, 179 (2003).

[26] G. Witte, K. Weiss, P. Jakob, J. Braun, K. L. Kostov, and C. Wöll, Phys. Rev. Lett. **80**, 121 (1998).

[27] M. Dion, H. Rydberg, E. Schröder, D. C. Langreth, and B. I. Lundqvist, Phys. Rev. Lett. **92**, 246401 (2004).

[28] H. Öström, D. Nordlund, H. Ogasawara, K. Weiss, L. Triguero, L. G. M. Pettersson, and A. Nilsson, Surf. Sci. **565**, 206 (2004).

[29] C. Kolczewski, R. Püttner, O. Plashkevych, H. Ågren, V. Staemmler, M. Martins, G. Snell, A. S. Schlachter, M. Sant'Anna, G. Kaindl, and L. G. M. Pettersson, J. Chem. Phys. **115**, 6426 (2001).

[30] P. S. Bagus, K. Hermann, and C. W. B., Jr., J. Chem. Phys. **80**, 4378 (1984).

[31] E. Wimmer, C. L. Fu, and A. J. Freeman, Phys. Rev. Lett. **55**, 2618 (1985).